TRANSIENT SUB-CRITICAL DROPLET EVAPORATION IN NON-ISOTHERMAL GASEOUS MIXTURES: EFFECTS OF RADIATION AND THERMAL EXPANSION

G. Ben-Dor, T. Elperin, B. Krasovitov

Department of Mechanical Engineering
The Pearlstone Center for Aeronautical Engineering Studies
Ben-Gurion University of the Negev, P.O.B. 653, Beer-Sheva 84105, Israel

ABSTRACT

In this study transient sub-critical evaporation of large droplet in non-isothermal stagnant gaseous mixtures taking into account the effects of radiation, liquid volumetric expansion and droplet heating is investigated numerically. System of transient nonlinear energy and mass conservation equations is solved using anelastic approximation. It was assumed that the droplet Biot number is small (Bi < 0.1) so that the temperature distribution inside the liquid droplet is uniform. The suggested model of droplet evaporation in non-isothermal gaseous mixtures at normal atmospheric pressure was applied to study the transient evaporation of large fuel droplets evaporating in hot gaseous multicomponent mixtures. Using the material balance at the droplet surface we obtained equations for the gaseous phase velocity (Stefan velocity) and the rate of change of the droplet radius taking into account liquid volumetric expansion. The boundary conditions taking into account the effect of liquid thermal expansion were obtained. It was found that in the case of sub-critical evaporation neglecting the liquid volumetric expansion causes underestimation of the evaporation rate at the initial stage and overestimation of the evaporation rate at the final stage of droplet evaporation. Also it is shown that increasing of the ambient temperature causes the larger droplet expansion at the initial stage of vaporization.

INTRODUCTION

Heat and mass transfer in dispersed systems is of interest in a wide range of atomization and sprays applications, e.g., spray combustion in furnaces, gas turbines, evaporative cooling, spray drying etc. Effect of droplet dilation during the initial stage of evaporation in a hot radiant gaseous mixture was considered in many studies on droplet high-pressure vaporization. High-pressure droplet evaporation models incorporate real gas effects, high-pressure phase equilibrium, dissolution of ambient gas in the droplet, liquid and gas phase pressure dependence of thermophysical properties [1], [2]. Computational modeling of complicated processes that include sub-critical droplet evaporation takes into account a number of physical phenomena (such as heat and mass transfer, droplet sedimentation, coagulation etc.) proceeding simultaneously. Since these numerical models require large calculations time, simplified models of large droplet ($Kn \ll 1$) evaporation [3–5] are used. Although numerous studies of droplet evaporation in the wide range of pressures [6], [7] were performed in the past, comprehensive model describing evaporation of droplets in the whole range of pressures is not developed as yet. The low-pressure models of droplet evaporation neglect the effect of liquid thermal expansion. In this study we demonstrated that the latter effect can be significant. In our study we considered transient evaporation of single fuel droplet immersed into the hot radiant ternary gaseous mixtures taking into account the effects of radiation absorption and thermal expansion.

MATHEMATICAL MODEL

Governing equations

Consider a spherical droplet with the initial radius R_0 immersed into the stagnant radiative gaseous mixture with temperature $T_{e,\infty}$. The droplet is heated by a conduction heat flux from the high temperature surroundings and begins to evaporate. In further analysis we assume spherical symmetry and neglect effects of buoyancy and thermal diffusion. Under these assumptions, the mass, species and energy conservation equations, describing the gaseous phase $r > R(t)$ surrounding the droplet read

$$r^2 \frac{\partial \rho}{\partial t} + \frac{\partial}{\partial r}\left(r^2 \rho v_r\right) = 0 \tag{1}$$

$$r^2 \frac{\partial}{\partial t}\left(\rho Y_j\right) + \frac{\partial}{\partial r}\left(\rho v_r r^2 Y_j\right) = \frac{\partial}{\partial r}\left(\rho D_i r^2 \frac{\partial Y_j}{\partial r}\right) \tag{2}$$

$$r^2 \frac{\partial(\rho c_p T_e)}{\partial t} + \frac{\partial}{\partial r}\left(\rho v_r r^2 c_p T_e\right) = \frac{\partial}{\partial r}\left(k_e r^2 \frac{\partial T_e}{\partial r}\right), \tag{3}$$

where t is the time, r is the radial coordinate, ρ is the density of gaseous mixture, v_r is the radial component of gas velocity, c_p is the specific heat at a constant pressure, $j = \overline{1, K}$ is the number of gaseous phase species (subscript 1 denotes volatile species), Y_j and M_j are the mass fraction and the molar mass of the j-th species, D_j is the diffusion coefficient, $D_j = (1 - X_j) / \sum\limits_{k \neq j}(X_k/D_{jk})$, X_j mole fraction of the j-th species, D_{jk} is the binary diffusion coefficient for species j and k, k_e and T_e are the coefficient of thermal conductivity of gaseous mixture and the temperature of gaseous phase surrounding.

For the liquid-phase region $r < R(t)$ the energy conservation equation reads:

$$\frac{\partial T_i}{\partial t} = \frac{1}{\rho_\ell c_\ell} \nabla(k_i \nabla T_i). \tag{4}$$

Since the Stefan velocity is much less then the sound velocity then for the solution of the system of heat and mass conservation equations instead of equation (1) we can use anelastic approximation [8]. Thus the radial flow velocity v_r reads

$$\rho v_r r^2 = -\frac{\dot{m}_\ell}{4\pi}, \tag{5}$$

where $\dot{m}_\ell$ is the mass rate of vaporization.

The gaseous phase properties can be related through the ideal gas equation of state:

$$p = p_\infty = \rho R_g T \sum_{j=1}^{K}\left(\frac{Y_j}{M_j}\right), \tag{6}$$

where R_g is the universal gas constant, p_∞ is the gaseous mixture pressure far from the droplet.

Since the problem under consideration involves moving boundaries, we transform a spatial coordinate system to a fixed domain where the receding droplet interface is immobilized. Introduce the following variables:

$$x = \frac{r}{R(t)}, \qquad \tau = \frac{\alpha_\ell t}{R_0^2}, \qquad \theta_e = \frac{T_e}{T_{e,\infty}}, \qquad \xi(\tau) = \frac{R(t)}{R_0}, \qquad \zeta_T = \frac{1}{\alpha_\ell \rho c_p}, \qquad \zeta_D = \zeta_T c_p.$$

Then the dimensionless energy and mass conservation equations for gaseous phase (2)–(3) read:

$$\xi^2 \frac{\partial \theta_e}{\partial \tau} - x\xi\dot{\xi}\frac{\partial \theta_e}{\partial x} + u\frac{\xi R_0}{\alpha_\ell}\frac{\partial \theta_e}{\partial x} = \frac{\zeta_T}{x^2}\frac{\partial}{\partial x}\left(x^2 k_e \frac{\partial \theta_e}{\partial x}\right) \tag{7}$$

$$\xi^2 \frac{\partial Y_j}{\partial \tau} - x\xi\dot{\xi}\frac{\partial Y_j}{\partial x} + u\frac{\xi R_0}{\alpha_\ell}\frac{\partial Y_j}{\partial x} = \frac{\zeta_D}{x^2}\frac{\partial}{\partial x}\left(x^2 \rho D_j \frac{\partial Y_j}{\partial x}\right), \tag{8}$$

where $j = \overline{1, K}$, $u = u(x, \tau)$ is the gas velocity and thermophysical properties ρ, D_j, k_e, and c_p are functions of the new independent variables x and τ.

Stefan velocity and droplet vaporization rate

Equations (7)-(8) must be supplemented by two equations for determining gas velocity $u = u(x, \tau)$ and $\dot{\xi}(\tau)$. The material balance at the droplet interface yields:

$$\frac{dm_\ell}{dt} = -4\pi R^2 \rho_s \left(v(R,t) - \dot{R}\right). \tag{9}$$

On the other hand the rate of evaporation reads:

$$\frac{dm_\ell}{dt} = \frac{d}{dt}\int\limits_{V(t)} \rho_\ell(r,t)dV, \tag{10}$$

where $\rho_\ell = \rho_\ell(r,t)$ is the material density of the droplet. Then after differentiating of the integral on the right-hand side of the equation (10) we obtain

$$\frac{dm_\ell}{dt} = \int\limits_V \frac{\partial \rho_\ell(r,t)}{\partial t}dV + 4\pi R^2 \rho_\ell(R,t)\dot{R}. \tag{11}$$

Choosing as independent variable the temperature within the droplet T_i in integrand expression in (11) and using energy conservation equation within the droplet (4) we obtain

$$\frac{dm_\ell}{dt} = -\int_V \frac{\eta}{c_\ell} \nabla(k_i \nabla T_i) dV + 4\pi R^2 \rho_\ell(R,t)\dot{R},$$

(12)

where $\eta = -\frac{1}{\rho_\ell}\left(\frac{\partial \rho_\ell}{\partial T_i}\right)_p$ is the coefficient of the liquid heat expansion, and c_ℓ is the specific heat of the liquid phase.

Taking into account that c_ℓ and η have only a weak dependence on temperature, after integrating the first term in the right-hand side of the equation (12), using (9) we obtain the following expression for the Stefan velocity

$$v_s = v_r(R,t) = \eta R \frac{\rho_{\ell,s}}{\rho_s} \frac{1}{3} \frac{dT_{i,s}}{dt} + \dot{R}\left(1 - \frac{\rho_\ell}{\rho_s}\right).$$

(13)

In the case of large size ($Kn \ll 1$) droplets at the gas-liquid interface the condition $T_i\big|_- = T_e\big|_+$ is fulfilled. Hereafter we will denote the temperature at the gas-liquid interface by T_s.

The molecules of the gaseous mixture species are not absorbed at the droplet surface. Using the impermeability condition and equations (9) and (13) it can easily be shown that

$$\dot{R} = \eta R \frac{\rho_{\ell,s}}{\rho_s} \frac{1}{3} \frac{dT_s}{dt} + \frac{\rho_s}{\rho_\ell} \frac{D_{1,s}(\partial Y_1/\partial r)\big|_{r=R}}{(1-Y_{1,s})}.$$

(14)

Then the dimensionless expressions for Stefan velocity and rate of change of droplet radius as functions of x and τ can be written as follows:

$$\dot{\xi}(\tau) = \frac{\rho_s}{\rho_{\ell,s}\xi} \frac{D_{1,s}(\partial Y_1/\partial x)\big|_{x=1}}{\alpha_\ell(1-Y_{1,s})} + \frac{\xi}{3} T_\infty \eta \frac{d\theta_s}{d\tau}, \qquad u_s = \frac{\alpha_\ell}{R_0}\dot{\xi}(\tau)\left(1 - \frac{\rho_{\ell,s}}{\rho_s}\right) + \frac{\xi}{3}\frac{\rho_{\ell,s}}{\rho_s}\frac{\eta T_\infty \alpha_\ell}{R_0}\frac{d\theta_s}{d\tau}$$

(15)

where $\alpha_\ell = k_i/(\rho_\ell c_\ell)$ is thermal conductivity of liquid and $\rho_\ell = \rho_{\ell,s} = \rho_\ell(\theta_s)$ is the function of droplet surface temperature.

Initial and Boundary conditions

The system of conservation equations (9)–(10) must be supplemented by initial conditions and the boundary conditions at the droplet surface. The initial conditions for the system of equations (9)–(10) read:

At $\tau = 0$ and $x = 1$ $\qquad\qquad\qquad\qquad\qquad \theta_e = \theta_0,$

(18)

For $x > 1$ $\qquad\qquad\qquad \theta_e = \theta_e^{(0)}(x), \qquad\qquad\qquad Y_j = Y_j^{(0)}(x).$

At the droplet surface the continuity conditions of the radial flux of volatile and gaseous species yield:

$$-\frac{1}{u}\frac{D_1}{\xi R_0}\frac{\partial Y_1}{\partial x}\bigg|_{x=1} = (1-Y_1)\big|_{x=1}, \qquad \frac{1}{u}\frac{D_j}{\xi R_0}\frac{\partial Y_j}{\partial x}\bigg|_{x=1} = Y_j\big|_{x=1}, \qquad (j = \overline{2,K}).$$

(19)

The value $Y_{1,s} = Y_1\big|_{x=1}$ at the droplet surface is determined using Clausius-Clapeyron equation:

$$Y_{1,s}(\theta_s) = \exp\left(-\frac{LM_1}{R_g T_b}\left(\frac{T_b}{\theta_s T_\infty} - 1\right)\right)$$

(20)

In the case when Biot number is small ($Bi < 0.1$) the temperature distribution inside the liquid droplet is uniform and time dependent. Under this assumption the droplet temperature can be found from the following equation [9]

$$\left(4\pi R^2 k_e \frac{\partial T_e}{\partial r}\right)\bigg|_{r=R} = \dot{m}_\ell L + \frac{4}{3}\pi R^2 \rho_\ell c_\ell \frac{\partial T_s}{\partial t} + 4\pi R^2(\mathbf{q}_R \cdot \mathbf{n}),$$

(21)

where $\mathbf{q}_R$ is the radiation flux vector. Then using equations (15) we can obtain the following dimensionless boundary condition

$$\frac{k_e}{k_\ell}\frac{1}{\xi}\left(\frac{\partial \theta_e}{\partial x}\right)\bigg|_{x=1} = -\frac{L}{c_\ell T_\infty}\frac{d\xi(\tau)}{d\tau}\bigg|_{x=1} + \frac{\xi}{3}\frac{d\theta_e}{d\tau}\bigg|_{x=1}\left(1 + L\frac{\eta}{c_\ell}\right) + \frac{R_0}{k_\ell T_\infty}Q_R,$$

(22)

where Q_R is heat flux due to radiation given by Stefan-Boltzmann law.

At $x \to \infty$ and $\tau > 0$ the 'soft' boundary conditions at infinity are imposed:

$$\frac{\partial \theta_e}{\partial x}\bigg|_{x\to\infty} = \frac{\partial Y_j}{\partial x}\bigg|_{x\to\infty} = 0, \qquad \left(j = \overline{1,K}\right).$$

(23)

3

NUMERICAL METHOD OF SOLUTION

The system of nonlinear parabolic partial differential equations (9)–(10) was solved using the method of lines [10]. The spatial discretization was performed using finite differences. The equations were approximated by a system of ordinary differential equations in time for the values θ_e and Y_j at the mesh points. The mesh points outside the droplet are spaced adaptively using the formula:

$$x_i = x_1 + (x_N - x_1)\left[1 - \cos\left(\frac{\pi}{2}\frac{(i-1)}{(N-1)}\right)\right] \tag{25}$$

so that they are clustered near the left boundary where gradients are steep. In Eq. (25) N is the chosen number of mesh points, x_1 and x_N are the locations of the left and right boundaries, respectively. The resulting system of ordinary differential equations is solved using backward differentiation method. Generally, in the numerical solution, 181 mesh points and an error tolerance $\sim 10^{-5}$ in time integration were employed. Variable time steps are used to improve the computing accuracy and efficiency. During numerical solution of the system of equations (7)–(8) the properties ρ, c_p, D_j, and k_e were evaluated simultaneously at each grid point for each iteration. The compilation of the formulas for calculations of these properties is presented in [8]. Calculations are terminated when the condition $R/R_0 \leq 0.1$ is fulfilled.

RESULTS AND DISCUSSION

The above model of transient sub-critical vaporization of large ($Kn \ll 1$) droplets in nonisotermal gaseous mixtures was applied to study evaporation of pure liquid droplets immersed into a stagnant radiative gaseous mixture. The numerical analysis of the effects of liquid volumetric expansion and thermal radiation was performed for n-heptane droplets with the radius 75 μm evaporating in pure nitrogen as well as in the gaseous mixtures involving the ternary combinations of N_2, CO_2, H_2O and n-C_7H_{16}-vapor gaseous species at atmospheric pressure.

The results of numerical calculations of the dependence of normalized droplet radius R/R_0 vs. dimensionless evaporation time τ, for n-heptane droplet with the initial radius 75 μm, initial temperature $T_0 = 274$ K and various values of the ambient temperature $T_{e,\infty}$ are shown in Fig. 1. The curves were plotted for the ambient temperatures $T_{e,\infty} = 800$, 600, and 500 K. The results were obtained for initial droplet temperature 274 K. The effect of thermal radiation was taken into account and the liquid density was calculated as a function of temperature. In this figure the solid and dashed lines are plotted for the cases of variable droplet density and constant droplet density approximation, correspondingly. The constant density was calculated at the initial temperature. As can be seen from Fig.1, in the case of sub-critical evaporation the effect of liquid volumetric expansion is pronounced and causes the decrease of droplet lifetime. The increase of the ambient temperature (see Fig. 1) causes the larger droplet expansion at the initial stage of vaporization. The dependences of the dimensionless radius and droplet surface temperature on dimensionless time τ are shown in Fig. 2. These results were obtained for the cases when: the effects of thermal expansion (variable ρ_ℓ) and radiation are taken into account (case 1); the effect of radiation is taken into account and liquid density is constant (case 2); the effect of radiation is neglected and liquid density is constant (case 3); and effect of thermal expansion is taken into account (variable ρ_ℓ) and radiation is neglected (case 4). Inspection of the Fig. 2 shows that taking into account the variable liquid density causes the decrease of droplet lifetime despite of the increase of the droplet diameter at the initial stage of vaporization. As can be seen from this plot neglecting the radiation effect causes an increase in droplet evaporation time.
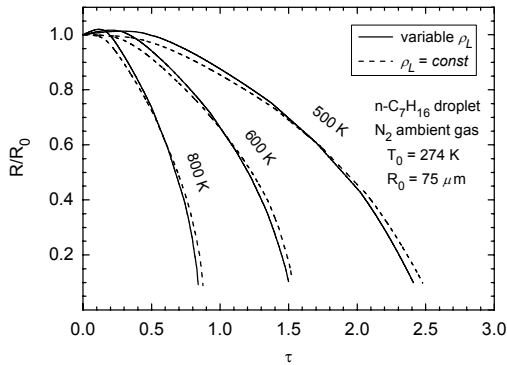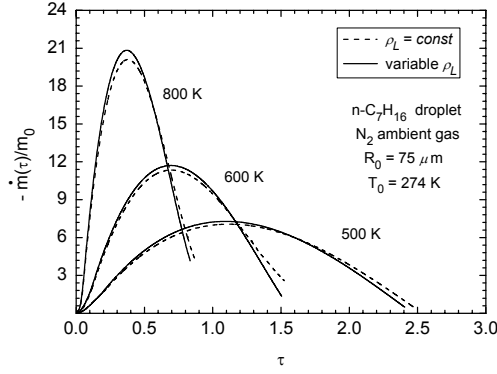

Fig. 1. Temporal evolution of the dimensionless radius of n-heptane droplet evaporating in nitrogen with the different ambient temperature.
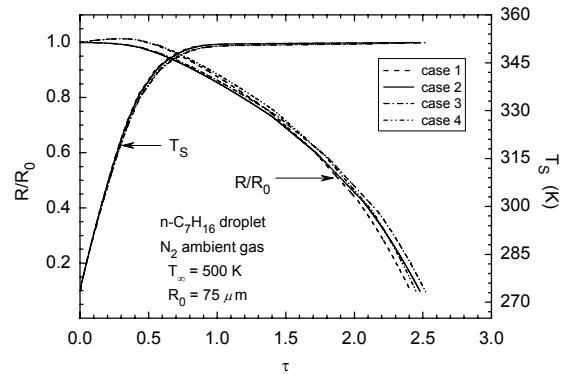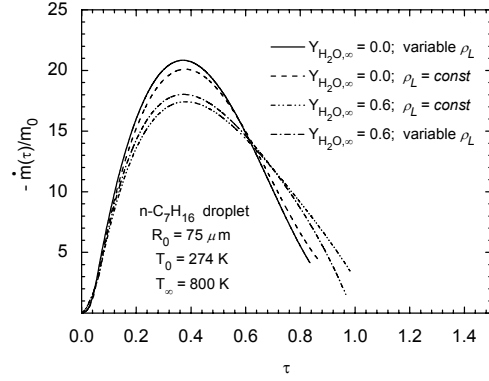

Fig. 2. Temporal evolution of the dimesionless radius and droplet surface temperature of n-heptane droplet evaporating in nitrogen.

Figure 3 shows the temporary variation of the dimensionless vaporization rate $-\dot{m}(\tau)/m_0$, where m_0 is the initial droplet mass. Calculations were performed for *n*-heptane droplet evaporating in pure nitrogen at pressure 1 atm and different ambient temperature (500, 600, and 800 K). In these as well as in the following calculations the effect of thermal radiation was taken into account. As can be seen from this plot neglecting liquid volumetric expansion causes underestimation of the vaporization rate at the initial stage and overestimation of the vaporization rate at the final stage of droplet evaporation (Fig. 3). With the presence of sufficiently large concentration of water vapor in the ambient N_2/H_2O gaseous mixture *n*-heptane droplet vaporization rate decreases significantly (Fig. 4) at the initial stage of evaporation. The reason is that the thermal conductivity of the water vapor at the temperature about 500 K and below is significantly less than thermal conductivity of nitrogen. Thus the presence of water vapor in nitrogen causes the significant decrease of the heat flux in the vicinity of the droplet and subsequent decrease of the *n*-heptane droplet vaporization rate.
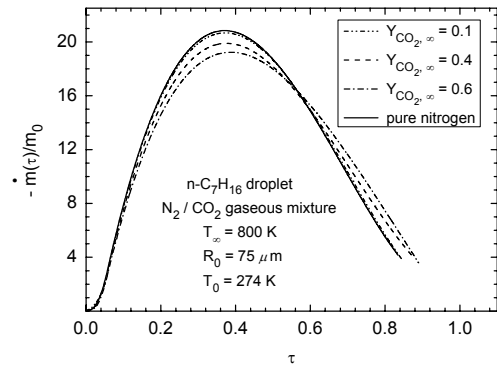

Fig. 3. Temporal evolution of the dimensionless vaporization rate of *n*-heptane droplet evaporating in nitrogen: solid lines variable droplet density approximation; dashed lines constant droplet density approximation.
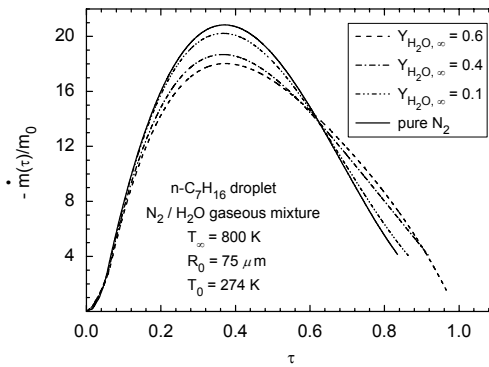
Fig. 4. Temporal evolution of the dimensionless vaporization rate of *n*-heptane droplet evaporating in N_2/H_2O-vapor gaseous mixture ($T_\infty = 800$ K).

The effect of water vapor and carbon dioxide concentration in ternary gaseous mixtures ($N_2/H_2O/C_7H_{16}$-vapor and $N_2/CO_2/C_7H_{16}$-vapor mixtures correspondingly) on the n-heptane droplet vaporization rate is showed in Figs. 5 and 6. Calculations were performed for the following values of CO_2 and water vapor mass fractions at infinity: 0.1, 0.4, and 0.6. The effects of liquid volumetric expansion and radiation were taken into account. As can be seen from Figs. 5 and 6 at the initial stage of evaporation carbon dioxide and water vapor species decrease the n-heptane vaporization rate and increase the droplet lifetime.

Fig. 5. Temporal evolution of the dimensionless vaporization rate of *n*-heptane droplet evaporating in N_2/CO_2 gaseous mixture ($T_\infty = 800$ K)

Fig. 6. Temporal evolution of the dimensionless vaporization rate of *n*-heptane droplet evaporating in N_2/H_2O-vapor gaseous mixture ($T_\infty = 800$ K)

CONCLUSIONS

Transient sub-critical evaporation of large droplet in non-isothermal stagnant gaseous mixtures taking into account the effects of radiation, liquid volumetric expansion and droplet heating was investigated numerically. System of transient nonlinear energy and mass conservation equations was solved using anelastic approximation. It was assumed that the droplet Biot number is small (Bi < 0.1) so that the temperature distribution inside the liquid droplet is uniform. The suggested model of droplet evaporation in non-isothermal gaseous mixtures at normal atmospheric pressure was applied to study the transient evaporation of a large fuel droplets evaporating in hot gaseous multicomponent mixtures. Using the material balance at the droplet surface we obtained equations for the gaseous phase velocity (Stefan velocity)

and the rate of change of the droplet radius taking into account liquid volumetric expansion. The boundary conditions taking into account the effect of liquid thermal expansion were obtained.

The numerical analysis of the effects of liquid volumetric expansion and thermal radiation was performed for n-heptane droplets with the radius 75 μm evaporating in pure nitrogen as well as in the gaseous mixtures involving the ternary combinations of N_2, CO_2, H_2O and n-C_7H_{16}-vapor gaseous species at atmospheric pressure. Two droplet vaporization models based on the variable and constant droplet density approximations were compared. It was found that in the case of sub-critical evaporation neglecting the liquid volumetric expansion causes underestimation of the evaporation rate at the initial stage and overestimation of the evaporation rate at the final stage of droplet evaporation. It is shown that the increasing of the ambient temperature causes the larger droplet expansion at the initial stage of vaporization.

Also it is shown that in the presence of sufficiently large concentration of water vapor in the ambient N_2/H_2O gaseous mixture n-heptane droplet vaporization rate decreases significantly at the initial stage of evaporation. The reason is that the thermal conductivity of the water vapor at the temperature about 500 K and below is significantly less than thermal conductivity of nitrogen.

NOMENCLATURE

Bi	Biot number		u, v	velocity [m/s]
c_p	specific heat at a constant pressure [J/kg · K]		X_j	mole fraction of the j-th species
D_j	diffusion coefficient of j-th species [m²/s]		Y_j	mass fraction of the j-th species

Greek symbols

D_{jk}	binary diffusion coefficient [m²/s]			
k	thermal conductivity [W/m · K]		α_ℓ	liquid thermal diffusivity [m²/s]
Kn	Knudsen number		η	coefficient of heat expansion [1/K]
L	latent heat of evaporation [J/kg]		ρ	density [kg/m³]
M_j	molar mass of j-th species [kg/mol]			

Subscripts and superscripts

m_ℓ	mass of the droplet [kg]		e	value outside a droplet
p	pressure [Pa]		i	value inside a droplet
r	radial coordinate [m]		j	number of species (1-st is the volatile species)
R	radius of the droplet [m]			
R_g	universal gas constant [J/mol · K]		ℓ	liquid
T	temperature [K]		s	value at the droplet surface
t	time [s]		∞	value at infinity

REFERENCES

1. F. Poplow, Numerical calculation of the transition from subcritical droplet evaporation to supercritical diffusion, *Int. J. Heat Mass Transfer*, vol. 37, No. 3, pp. 485–492, 1994.
2. G.-S. Zhu, R. D. Reitz and S. K. Aggarwal, Gas-phase unsteadiness and its influence on droplet vaporization in sub- and super-critical environments, *Int. J. Heat and Mass Transfer*, vol. 44, pp. 3081–3093, 2001.
3. G. A. E. Godsave, Studies of the Combustion of drops in a fuel spray – the burning of single drops of fuel, *Fourth Symposium (International) on Combustion*, Williams & Wilkins, Baltimore, pp. 818–830, 1953.
4. D. B. Spalding, *The combustion of liquid fuels, Fourth Symposium (International) on Combustion*, Williams & Wilkins, Baltimore, pp. 847–864, 1953.
5. B. Abramzon, W. A. Sirignano, Droplet vaporization model for spray combustion calculations, *Int. J. Heat and Mass Transfer*, vol. 32, No. 9, pp. 1605–1618, 1989
6. L. Consolini, S. K. Aggarwal, S. Murad, A molecular dynamics simulation of droplet evaporation, *Int. J. Heat and Mass Transfer*, vol. 46, pp. 3179–3188, 2003.
7. K. Harstad, J. Bellan, An all-pressure fluid drop model applied to a binary mixture: heptane in nitrogen, *Int. J. Multiphase Flow*, vol. 26, pp. 1675–1706, 2000.
8. G. Ben-Dor, T. Elperin, B. Krasovitov, Effect of thermo- and diffusiophoretic motion of flame-generated particles in the neighbourhood of burning droplets in microgravity conditions, *Proceedings of the Royal Society London* A 459, pp. 677–703, 2003.
9. I. Glassman, *Combustion*, 2nd ed., Academic Press, London, 1987.
10. R. F. Sincovec, N. K. Madsen, Software for nonlinear partial differential equations, *ACM Transactions on Mathematical Software*, vol. 1, pp. 232–260, 1975.